which are involved in attempts to calculate atomic force constants from first principles.[28] It seems likely that a systematic study of impurity systems will reveal interesting correlations even in the absence of such detailed analysis.

[28] H. C. White, Phys. Rev. **112**, 1092 (1958).

ACKNOWLEDGMENTS

We would like to acknowledge helpful discussions with Dr. K. K. Singh and with Professor B. R. A. Nijboer. One of us (RMH) would like to express his sincere thanks to Professor H. de Waard for making his stay at Groningen possible.

PHYSICAL REVIEW VOLUME 146, NUMBER 2 10 JUNE 1966

Temperature Dependence of Infrared Dispersion in Ionic Crystals LiF and MgO*

J. R. JASPERSE†, A. KAHAN, AND J. N. PLENDL
Air Force Cambridge Research Laboratories, Office of Aerospace Research, Bedford, Massachusetts

AND

S. S. MITRA‡
Physics Research Division, IIT Research Institute, Chicago, Illinois

(Received 27 December 1965)

Infrared-reflectivity measurements were made from 200 cm^{-1} to 800 cm^{-1} at temperatures ranging from 7.5 to 1060°K for LiF and from 8 to 1950°K for MgO. The reflection spectra were analyzed by means of a two-resonance damped-oscillator model, and the calculated optical properties are presented. Dielectric dispersion theory is reviewed and it is shown that all the major theories discussed give identical results for the susceptibility when evaluated at the reststrahlen frequency but differ from one another at other frequencies. The damping constant γ for LiF and MgO in the high-temperature limit ($h\nu_1 < kT$) agrees reasonably well with the formula suggested by Maradudin and Wallis, but discrepancies seem to appear in the low-temperature limit ($h\nu_1 > kT$). The general behavior of the extinction coefficient in the wings of the absorption region is consistent with the notion of continuous absorption produced by multiphonon processes. The shift of the long-wavelength optical-mode frequencies of LiF, MgO, and RbI with temperature is discussed in terms of the volume and other anharmonic effects. The anharmonic part of the frequency shift is found to agree qualitatively with the theory of Maradudin and Fein.

I. INTRODUCTION

IN this paper the infrared reflection spectra of single-crystal LiF and MgO are presented as functions of temperature ranging from 7.5°K to near their respective melting points. The experimental work was motivated by the fact that very few self-consistent measurements of the infrared reflectivity have been made for such wide temperature ranges. By using a two-resonance damped-oscillator model, numerical values for the high and low-frequency dielectric constants, long-wavelength optic-mode frequencies and damping constants are obtained as functions of temperature. The results are discussed in relation to the existing theoretical models used to represent the dielectric constant. The relationship between the experimentally determined dielectric constant in the infrared for an ionic crystal and that predicted by theory has been extensively discussed in the literature. A brief review of the theoretical models for representing the dielectric constant of ionic crystals is presented here. The width and shift of the one-phonon frequencies with temperature are discussed in the light of existing lattice dynamical theories of ionic crystals incorporating anharmonic forces.

II. EXPERIMENTAL PROCEDURE

Infrared-reflectivity measurement at low and high temperatures were made using a Perkin-Elmer Model 12 monochromator equipped with a cesium bromide and a cesium iodide prism. A special fore-optical system was designed and built such that both a low- and high-temperature cell could be attached to the spectrometer. The entire system was enclosed in a thick-walled plexiglass housing and could be continuously flushed with a dry inert gas. For measurements at liquid-nitrogen temperatures and above, dry nitrogen was used to flush the spectrometer. At liquid-helium temperatures high-purity helium gas was used. The reflectivities were determined by a measurement of the

* Parts of this paper were presented at the Eighth European Congress on Molecular Spectroscopy, held in Copenhagen, Denmark, August 15–20, 1965, and the American Physical Society Meeting held in Honolulu, Hawaii, September 2, 1965. Some of the preliminary data were published in Appl. Phys. Letters, Vol. 5, No. 2 (1964).

† The experimental work and some of the analytical work was done by J. R. Jasperse while at Arthur D. Little, Inc., Cambridge, Massachusetts under contract with U. S. Air Force Cambridge Research Laboratories, Office of Aerospace Research.

‡ The analytical work done by S. S. Mitra was also supported by U. S. Air Force Cambridge Research Laboratories, Office of Aerospace Research.

radiation reflected from the sample at a given frequency compared to that reflected by an aluminized mirror at the same frequency. The reflectivity of the aluminized mirror from 200 to 800 cm^{-1} was taken to be 98.5%. The average angle of the incident light beam was 11 deg from the normal to the crystal surface. Chopping of the infrared flux was accomplished by several crystal choppers ahead of the sample area in the optical path, so that the background infrared radiation from the heated sample would appear at the detector as a constant flux. Black polyethylene transmission filters were also used to reduce the amount of near infrared radiation. Calcium fluoride and sodium chloride transmission filters were inserted and withdrawn from the optical path during each measurement in order to measure the scattered radiation.

The high-temperature cell was mounted beneath the horizontal plane of the fore-optics and monochromator. The single crystals of LiF and MgO were held in a platinum disc-shaped holder and mounted at the center of a radio-frequency induction coil. The samples were heated by a 1.5-kW Sylvania power supply coupled to the platinum holder. Sample temperatures of 1950°K for MgO were easily achieved using this technique. Sample surface temperatures were measured with an optical pyrometer above incandescence and with a Chromel-Alumel thermocouple imbedded in the sample holder for the lower temperatures. The calibration procedures will not be discussed here, but we feel that the temperatures reported in this paper are accurate to within ±2% of the absolute value. Thermal gradients across the diameter of the sample at the higher temperatures were studied and found to be within experimental error. The high- and low-temperature cells were constructed to allow fine adjustments of the crystal-surface orientation during measurements.

The low-temperature cell consisted of a specially designed double-wall dewar capable of operating at liquid-helium temperatures without infrared windows. Sample temperatures measured by two gold −2.1 at.% cobalt versus copper thermocouples should be accurate within ±2–3°K.

High-purity, single crystals of LiF and MgO were cut and hand polished until they were optically flat to about $\frac{1}{2}$-wave at the sodium d line. The samples were then annealed in a vacuum furnace for two days at a temperature of about $\frac{3}{4}$ of the melting temperature of the crystal. Reflectivity data were checked several times for different samples of the same material, for several cycles of heating and cooling, and reproduced under all these conditions to within ±1 to ±2%. The calculated resolution of the spectrometer was found to vary from about 2 cm^{-1} at 800 cm^{-1} to about 4 cm^{-1} at 220 cm^{-1}.

III. DATA PRESENTATION

A. Methods of Calculation

The application of classical-oscillator theory to the analysis of the lattice-vibrational spectra of solids has been extensively reviewed and discussed.[1–4] It is possible that the classical pole-fit procedure may not represent the exact dielectric constant as a function of frequency and temperature even for alkali-halide crystals. However, the pole-fit procedure is useful for obtaining some information about the optical properties of alkali halides. These questions are discussed in Sec. IV. The relevant equations for the real and imaginary parts of the complex dielectric constants according to a classical oscillator analysis are

$$\epsilon' = n^2 - k^2 = \epsilon_\infty + \sum_j \frac{4\pi\rho_j \nu_j^2(\nu_j^2 - \nu^2)}{(\nu_j^2 - \nu^2)^2 + (\gamma_j \nu)^2} \tag{1}$$

and

$$\epsilon'' = 2nk = \sum_j \frac{4\pi\rho_j \nu_j^2(\gamma_j \nu)}{(\nu_j^2 - \nu^2)^2 + (\gamma_j \nu)^2}, \tag{2}$$

where ϵ_∞ is the high frequency dielectric constant, $4\pi\rho_j$ the strength, γ_j the damping constant and ν_j the frequency of the jth resonance. The reflectivity R of unpolarized radiation at normal angle of incidence is related to the refractive index n and extinction coefficient k by

$$R = ((n-1)^2 + k^2)/((n+1)^2 + k^2). \tag{3}$$

The classical-oscillator-analysis computer program that we used includes angle of incidence effects and was described in another publication.[5]

The analysis procedure is as follows: From the experimental reflectivity curve to be fitted, one selects a number of points which are to be approximated within a prescribed tolerance. In our case we chose approximately 20 points with $\Delta R \leqslant 0.02$. Input requirements include a series of values for each parameter, number of oscillators, experimental angle of incidence, and frequency ranges and intervals of interest. For the first combination of input parameters, the program calculates the reflectivity at the frequency of the first test point. If the computed value is within the specified deviation the program will proceed to calculate the reflectivity at the second test point, and so on. If the reflectivity value at any test point does not meet the requirements, the program continues to the next combination of parameters, until it completes the calculations over all sets of input parameters. For further details concerning the computer program, see Ref. 5.

Our initial efforts to calculate the optical constants by the Kramers-Kronig (K-K) method encountered difficulties similar to the ones experienced by Schatz

[1] S. S. Mitra and P. J. Gielisse, *Progress in Infrared Spectroscopy* (Plenum Press, Inc., New York, 1964), Vol. 2, pp. 47–125.
[2] F. Stern, *Solid State Physics*, edited by F. Seitz and D. Turnbull (Academic Press Inc., New York, 1963), Vol. 15, p. 351.
[3] W. G. Spitzer and D. A. Kleinman, Phys. Rev. **121**, 1324 (1961).
[4] E. Burstein, *Phonon and Phonon Interactions*, edited by T. A. Bak (W. A. Benjamin, Inc., New York, 1964), p. 276.
[5] A. Kahan (to be published).

et al.,[6] Bowlden,[7] Gottlieb,[8] and Sanderson.[9] However, with further modifications, we were able to generate extinction curves by the K-K method which agreed reasonably well with the results of the pole-fit, except on the low frequency side of the main resonance. We found that a shift of 0.02 in the far-infrared value of the reflectivity could induce negative absorption coefficients, shift the position of the maximum by 3–4 wave numbers, and change the maximum value of k by 10 to 15%. The results presented in this paper are based on classical oscillator theory and not on K-K relations.

B. Results and Discussion of the Reflectivity for LiF and MgO

The reflection spectra from 200 to 800 cm^{-1} of the polished, annealed, single crystals of LiF and MgO are

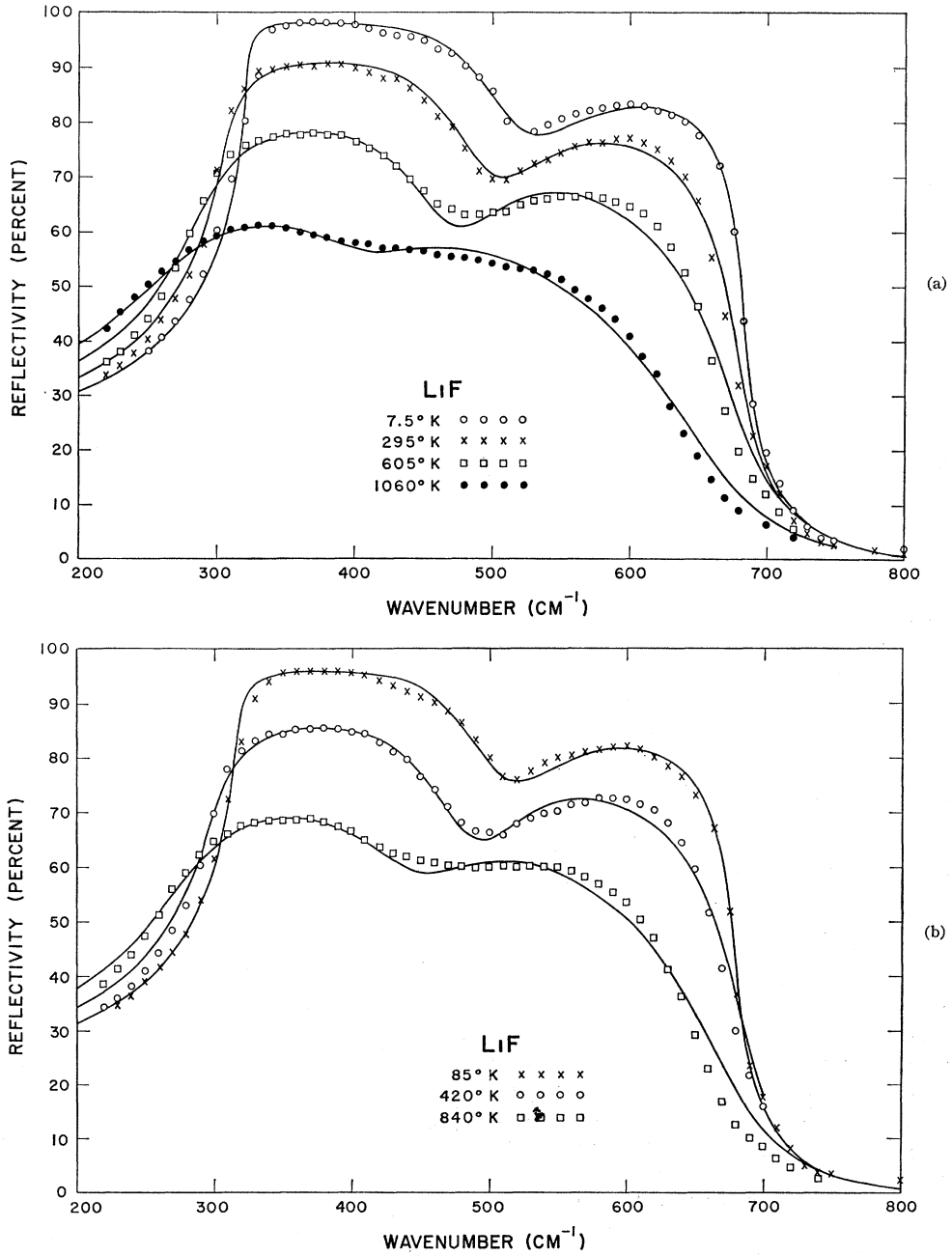

FIG. 1. Infrared reflectivity of LiF as a function of wave number and temperature. The various symbols are experimental points and the solid lines are the theoretical curves calculated from the dispersion parameters of Table I.

[6] P. N. Schatz, S. Maeda, and K. Kozima, J. Chem. Phys. 38, 2658 (1963).
[7] H. J. Bowlden and J. K. Wilmhurst, J. Opt. Soc. Am. 53, 1073 (1963).
[8] M. Gottlieb, J. Opt. Soc. Am. 50, 343 (1960).
[9] R. B. Sanderson, J. Phys. Chem. Solids 26, 803 (1965).

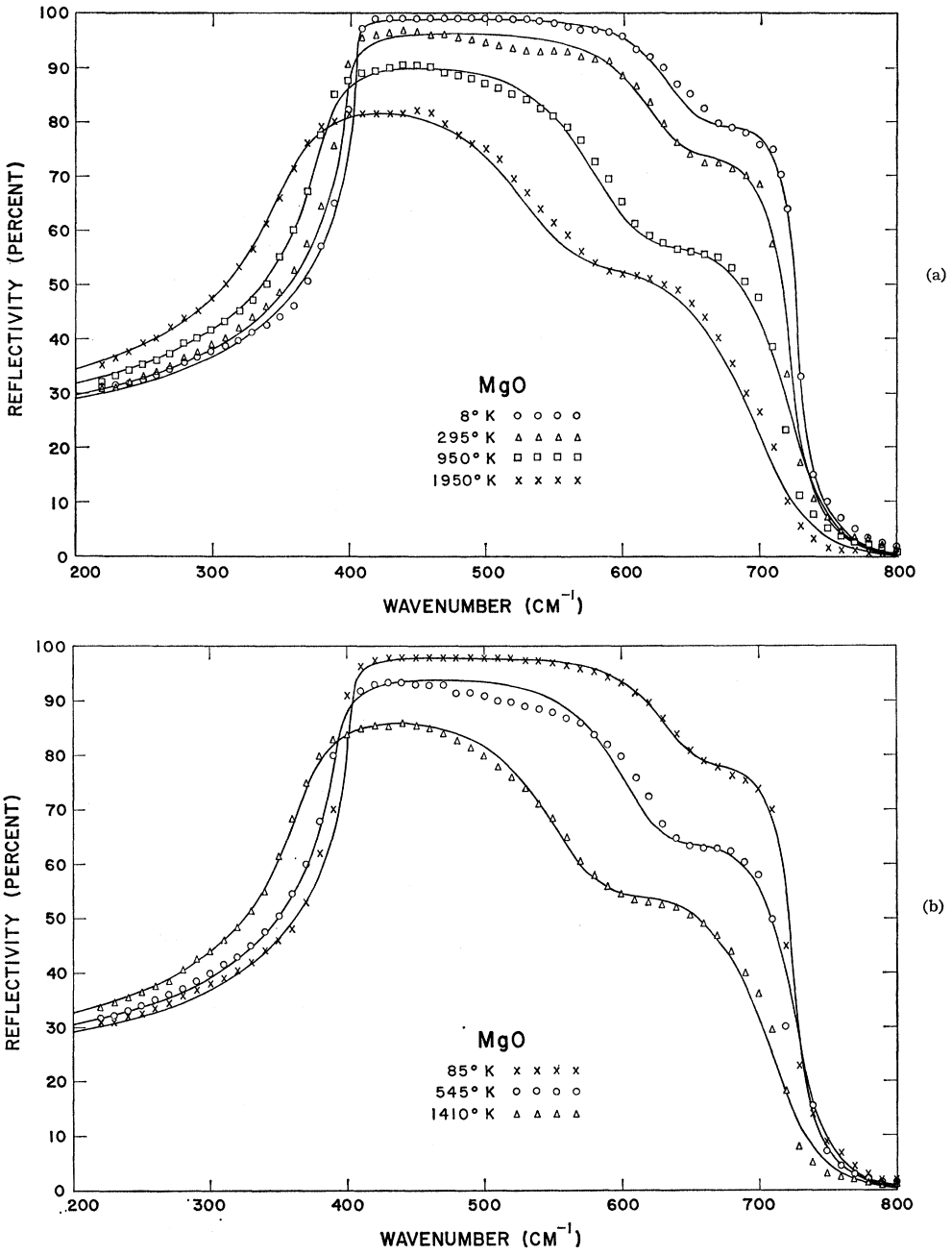

FIG. 2. Infrared reflectivity of MgO as a function of wave number and temperature. The various symbols are experimental points and the solid lines are the theoretical curves calculated from the dispersion parameters of Table II.

shown as a function of temperature in Figs. 1 and 2. We note that as the temperature increases, the intensity of the main band and side band decreases, and the reflection band shifts to lower wave numbers. For both materials the fundamental resonance occurs at lower wave numbers, and a subsidiary peak at the higher wave numbers. In most regions of the spectrum good agreement between the pole-fit and experiment was achieved. The greatest discrepancies occur in areas of reflectivity shoulders and steep slopes, regions corresponding to least accurate experimental results. The pole-fit results represent the best average correlations which can be obtained for a two-resonance model. Improved agreement in a particular region of the spectrum can be attained only at the expense of drastic changes at other frequencies.

All reflectivity-curve fits for MgO were accomplished with comparative ease, but not so for the high-temperature data on LiF. For the latter even the inclusion of a third oscillator did not improve the fit. The calculated dispersion parameters of the theoretical reflectivity curves are shown in Tables I and II, and some are

TABLE I. Infrared-dispersion parameters and related quantities for LiF. $\epsilon_\infty = 1.90 \pm 0.02$ (temperature-independent).

Temp. °K	ν_1 cm^{-1}	ν_2 cm^{-1}	γ_1/ν_1	γ_2/ν_1	$4\pi\rho_1$	$4\pi\rho_2$	ϵ_0	ν_l (cm^{-1}) $\epsilon'=0$	LST
7.5	320±1	520±3	0.0100±0.006	0.185±0.010	6.10±0.05	0.085±0.005	8.09	672	660
85	315	512	0.0225	0.180	6.30	0.090	8.29	670	658
295	306	503	0.0600	0.180	6.80	0.110	8.81	672	659
420	301	497	0.1000	0.180	7.20	0.125	9.23	675	663
605	293	486	0.1700	0.170	7.65	0.130	9.68	674	661
840	282	462	0.2750	0.210	8.25	0.140	10.29	664	656
1060	271±2	430±5	0.3850±0.015	0.245±0.020	8.70±0.16	0.160±0.02	10.76	646	645

TABLE II. Infrared-dispersion parameters and related quantities for MgO. $\epsilon_\infty = 3.01$ (temperature-independent).

Temp. °K	ν_1 cm^{-1}	ν_2 cm^{-1}	γ_1/ν_1	γ_2/ν_2	$4\pi\rho_1$	$4\pi\rho_2$	ϵ_0	ν_l (cm^{-1}) $\epsilon'=0$	LST
8	408	653	0.0045	0.140	6.30	0.025	9.34	724	719
85	406	650	0.0100	0.145	6.40	0.030	9.44	725	719
295	401	640	0.0190	0.160	6.60	0.045	9.64	725	718
545	394	630	0.0325	0.170	6.75	0.075	9.84	724	712
950	382	610	0.0570	0.195	7.10	0.120	10.23	720	705
1410	368	590	0.0850	0.225	7.45	0.175	10.64	711	692
1950	355	566	0.1200	0.260	7.95	0.225	11.19	703	685

plotted in Figs. 3 to 5. The parameters characterizing the oscillators are smoothly varying functions of temperature.

The errors involved in the computed dispersion parameters were evaluated for LiF at low and high temperatures and are indicated in Table I. When the parameters are varied one at a time, these deviations will induce either a $\Delta R \leq 0.01$ in the flat portions of the reflectivity spectrum or a $\Delta\nu \leq 3$ cm^{-1} in the regions of high slope. The absolute value of the reflectivity decreases with increasing temperature and correspondingly, the derived parameters become less sensitive to error. The relative accuracies of the MgO oscillators (not shown in the Table) follow a similar pattern. However, none of these resonances is unique: for example, a shift in ν_1, can be balanced by a corresponding change in either $4\pi\rho_1$ or ϵ_∞, and a deviation in ν_2 can be restored by modifying $4\pi\rho_2$. The errors in γ_1 due to a $\Delta R = 0.01$ in the maximum reflectivity value, is denoted in Fig. 5 at each measured temperature by a vertical bar. We note that the relative accuracy of γ_1 decreases as the reflectivity amplitude approaches unity.

For both materials we assume a temperature-independent high-frequency dielectric constant. In the initial phases of our computations we allowed ϵ_∞ to be temperature dependent. We found that this effect could be balanced by a systematic shift in the ν_1 values, so, in the absence of accurate measurements of $\epsilon_\infty(T)$, we neglected this effect in subsequent calculations. The relative shift in ϵ_∞ with temperature was experimentally determined and found to be so slight that it could be assumed constant for the purposes of a pole fit. Far

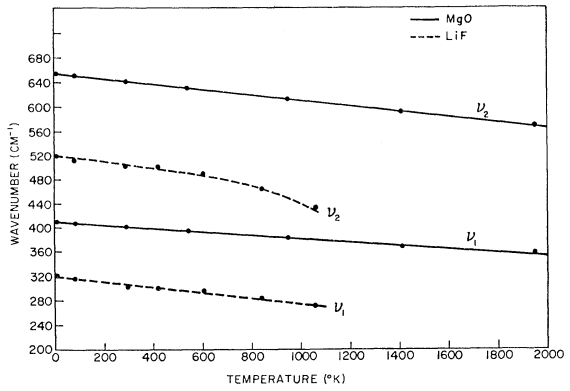

FIG. 3. Temperature dependence of the resonance frequencies for LiF and MgO.

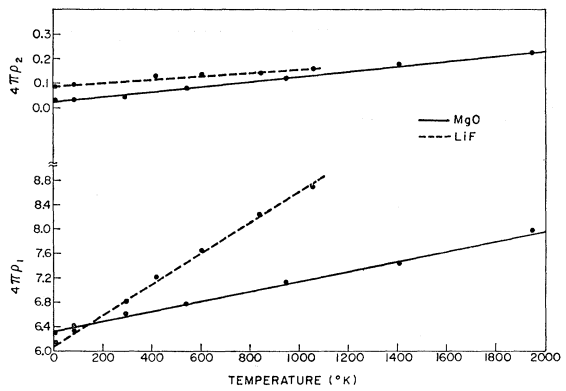

FIG. 4. Temperature variation of the strength of the main and secondary resonance for LiF and MgO.

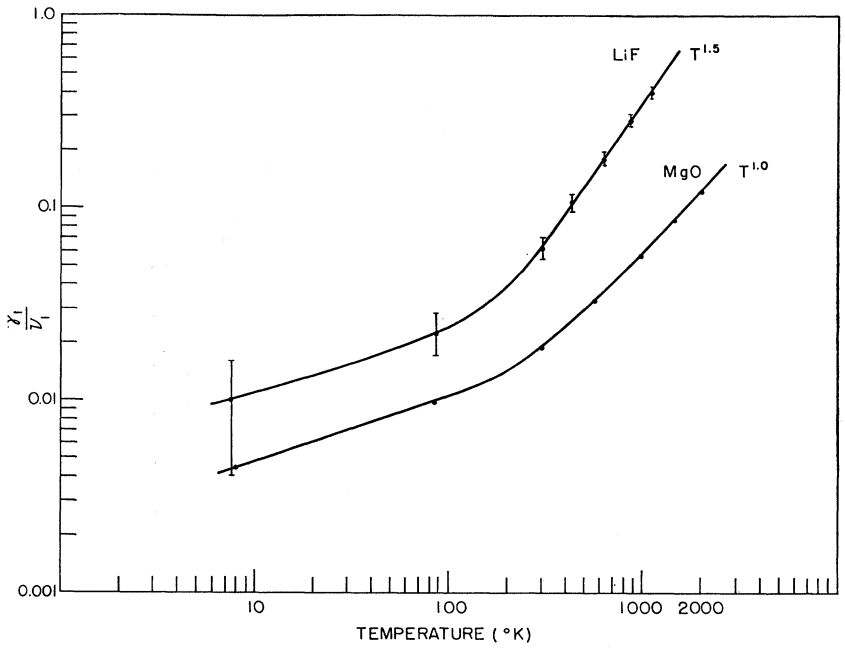

FIG. 5. The damping constant of the main band as a function of temperature. The vertical lines correspond to a $\Delta R=0.01$ in the value of the maximum reflectivity.

infrared transmission measurements on LiF by Klier[10] and by Seger and Genzel[11] indicate a difference band centered around 110 μ. Our reflectivity measurements do not extend into the far-infrared, but presumably the strength of this difference band is such as to have some effect on the reflectivity values. Therefore, the values of the low-frequency dielectric constant ϵ_0 will be underestimated if calculated from the parameters shown in Table I, unless a third oscillator at 110 μ is added.

For LiF the frequency of the main resonance ν_1 at room and at liquid-nitrogen temperatures is fairly well established from transmission[12] measurements and is in agreement with our results. For MgO, Piriou[13,14] measured the infrared reflectivity at temperatures of 293, 1080, and 2225°K, and by a K-K analysis calculated the optical constants and some of the dispersion parameters. His ν_1 values agree with ours within experimental and computational error. γ_1 also coincides at higher temperatures but differs slightly at room temperature. This can be attributed to a small difference in the maximum reflectivity at room temperature.

Berreman[15] developed a method of calculating the longitudinal optical (LO) mode of the lattice near the center of the Brillouin zone from transmission measurements on thin films at non-normal angles of incidence. Here, the frequency of the LO mode is defined as the position where the real part of the complex dielectric constant vanishes and may also be approximately calculated from the Lyddane-Sachs-Teller formula. For LiF at room temperature, Berreman observes this frequency to be 670 ± 2 cm^{-1}. Our computations show this frequency to be 672 cm^{-1}. In addition, both the shape and absolute values of the absorption factor $\epsilon''/\epsilon'^2+\epsilon''^2$ between 600–750 cm^{-1} are in excellent agreement with Berreman's experimental results. It is surprising that our correlation is better than the one shown by Berreman based on the frequency-dependent damping factor of Bilz, Genzel, and Happ.[16] Berreman also obtained good agreement for CaF_2 using a constant γ.

C. The Calculated Optical Constants for LiF and MgO

Figures 6(a) and (b) and Figs. 7(a) and (b) show, respectively, the calculated refractive indices and extinction coefficients of LiF and MgO as a function of temperature and wavenumber. For both materials we plot the two extreme temperatures, and for clarity omit some of the in-between curves. As the temperature increases, the optical constant curves broaden, the maxima decrease and shift to lower frequencies. As can be seen in the enlarged scale portion of Fig. 6, the second oscillator produces a peak in the n value, but no perceptible effect is evidenced for k from the pole fit.

Figures 8(a) and (b) and Figs. 9(a) and (b) show the real and imaginary parts of the dielectric constant as a function of wave number. Again, their temperature

[10] M. Klier, Z. Physik **150**, 49 (1958).
[11] G. Seger and L. Genzel, Z. Physik **169**, 66 (1962).
[12] E. E. Bell and R. L. Brown, Ohio State University Report, AFRCRC-TN-60-260 (unpublished).
[13] B. Piriou, Compt. Rend. **259**, 1052 (1964).
[14] B. Piriou, Compt. Rend. **260**, 841 (1965).
[15] D. W. Berreman, *Proceedings of International Conference on Lattice Dynamics, Copenhagen, 1963* (Pergamon Press, Inc., 1965), p. 397; Phys. Rev. **130**, 2193 (1963).
[16] H. Bilz, L. Genzel, and H. Happ, Z. Physik **160**, 535 (1960).

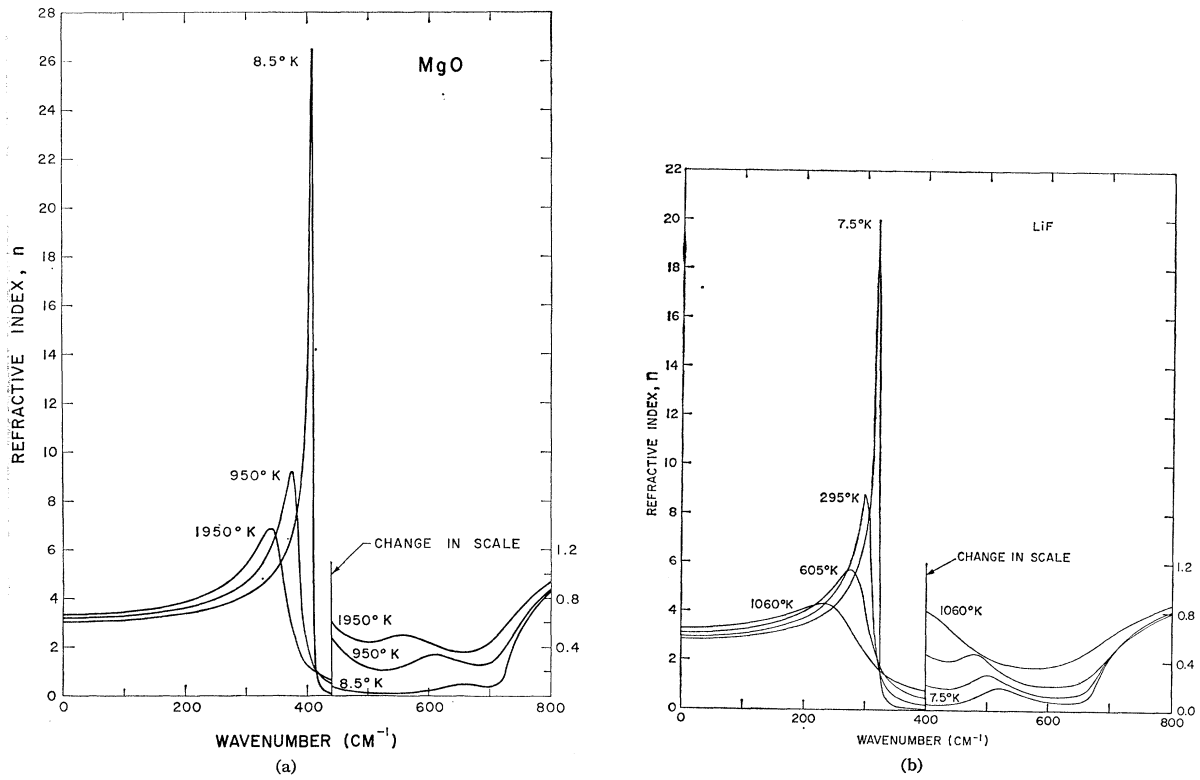

FIG. 6. Calculated refractive indices of LiF and MgO as function of wave number and temperature (note change in vertical scale).

behavior is similar to the optical constants, but the effects of the second resonance are more noticeable in ϵ''. Figures 10(a) and (b) show the related absorption coefficients ($\alpha=4\pi\nu k$) from 100 to 800 cm^{-1}. These curves amplify the absorption characteristics of the material in regions of small k.

All methods, whether classical oscillator theory, K-K analysis, or reflectivity measurements at two angles of incidence, when applied in calculating the refractive indices and extinction coefficients of a material, involve the basic Fresnel equations connecting the reflectivity with n and k. The calculated value for the index of refraction of LiF at $T=85°K$, corresponding to $R=0.96$, is $n_{max}=13.58$ and for $R=0.97$ we get $n_{max}=15.70$, a difference of 13.5%. Hence, when the reflectivity value is near unity, the accuracy of the optical constants is $\pm$10–15%. The precision of the calculations improve with decreasing reflectivity. For LiF at $T=1060°K$, a ΔR of 0.01, equivalent to a 1.6% deviation, introduces a 1.4% error in the calculated maximum value of the refractive index. Therefore, when comparing results of different investigators obtained by different experiments and methods of calculation, one must evaluate the accuracies involved in the calculated optical constants.

The different results for reflectivity and optical constants obtained by Heilmann,[17] Bell and Brown,[12] and Gottlieb,[8] for LiF at low temperatures prompted Frohlich[18,19] to repeat these experiments and evaluate the results of the previous investigators. He suggests various possibilities for the disagreements, and lists the shortcomings in the experimental procedures of the other investigators. Our reflectivities and optical constants are in agreement, within experimental and computational accuracies, with the values obtained by Frohlich. On the low- and high-frequency side of the maximum there is close correlation, whereas at the center of the resonance the differences in the n and k values are well within computational accuracies.

Klier[10] measured the transmission of LiF and calculated k for both the low- and high-frequency sides of the main resonance, and also found an additional band centered around 110 μ. At room temperature and at 575°K our calculated absorption curves are in general agreement with his work, when the effects of the third resonance are subtracted out. But, at liquid-nitrogen temperatures the absolute value of our extinction coefficient is an order of magnitude higher. However, one must be very cautious when comparing to the results of Klier. The formulas applied by Klier to calculate k are highly simplified ones, and the condition for their applicability should be very carefully evaluated.[20] In

[17] G. Heilmann, Z. Physik **152**, 368 (1958).

[18] D. Frohlich, Z. Physik **169**, 114 (1962).

[19] D. Frohlich, Z. Physik **177**, 126 (1964).

[20] A. Kahan and H. G. Lipson, Air Force Cambridge Research Laboratory Report, AFCRL-63-325 (unpublished).

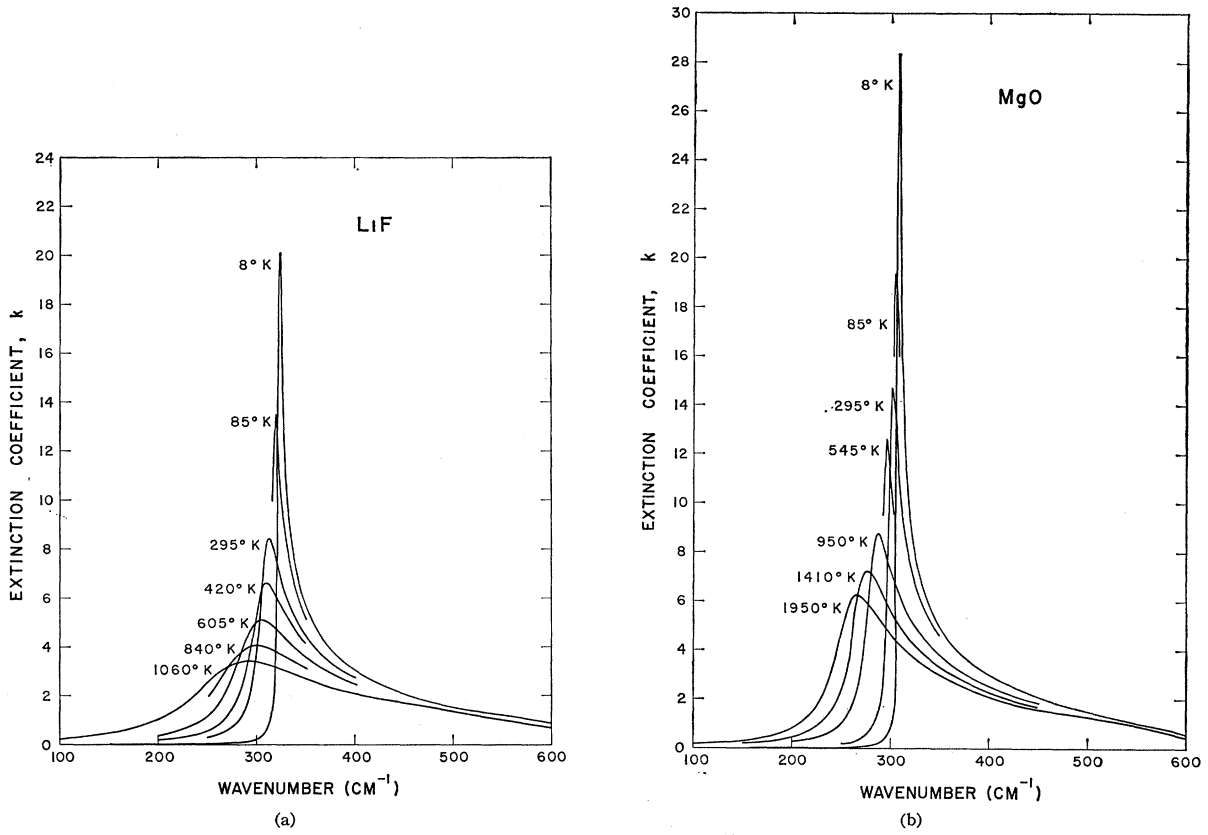

FIG. 7. Computed extinction coefficients of LiF and MgO as function of wave number and temperature.

a later work, Seger and Genzel[11] repeated the room-temperature measurements on an interference-type spectrometer, and re-determined k. They also show the best combined experimental curve for k from the near-infrared to 1000 μ. Aside from the third resonance which can be subtracted out, our calculated values are in reasonably good agreement with their combined curve.

IV. COMMENTS ON DIELECTRIC DISPERSION THEORY

According to classical dispersion theory it is assumed that the dielectric constant of an ionic crystal may be represented by Eqs. (1) and (2). The sum here is intended to include all poles necessary to represent the dielectric constant. We wish to emphasize that classical dispersion theory is, in reality, a conjecture and may or may not represent the real dielectric constant. It is useful, in part, because it has a simple form, and, with the aid of a computer, the optical constants n and k may easily be calculated. The Kramers-Kronig equations, however, express an exact relationship between the real and imaginary parts of the dielectric constant and does not assume a model for calculating ϵ. This may be derived as a direct consequence of the principles of causality and the fact that the dielectric constant must be an analytically continued function in the complex frequency domain.[21] We also wish to note that the K-K relations impose a much more general and less restrictive condition on ϵ than those embodied in the pole fit. In practice, however, it appears that the pole-fit procedure actually represents the experimental reflectivity to a reasonable degree of accuracy even for crystals which require a large number of poles.[3] It also turns out that the Kramers-Kronig relation is sometimes not useful in determining the full-frequency dependence of one part of ϵ from the other part, because of the errors involved in calculating the phase from the magnitude of the reflectivity.

In quantum-mechanical dispersion theory the philosophy is quite different from that of the classical pole-fit procedure. Here, one calculates the detailed form of the dielectric constant from a particular Hamiltonian representing the crystal and the incident electromagnetic field. From the Hamiltonian one computes the equations of motion for the ions composing the crystal and hence the induced polarization caused by the electromagnetic field. One may then calculate the electric susceptibility tensor $\chi_{\mu\nu}$ by some approximation technique and write the dielectric constant in

[21] M. Sharnoff, Am. J. Phys. 32, 1 (1964).

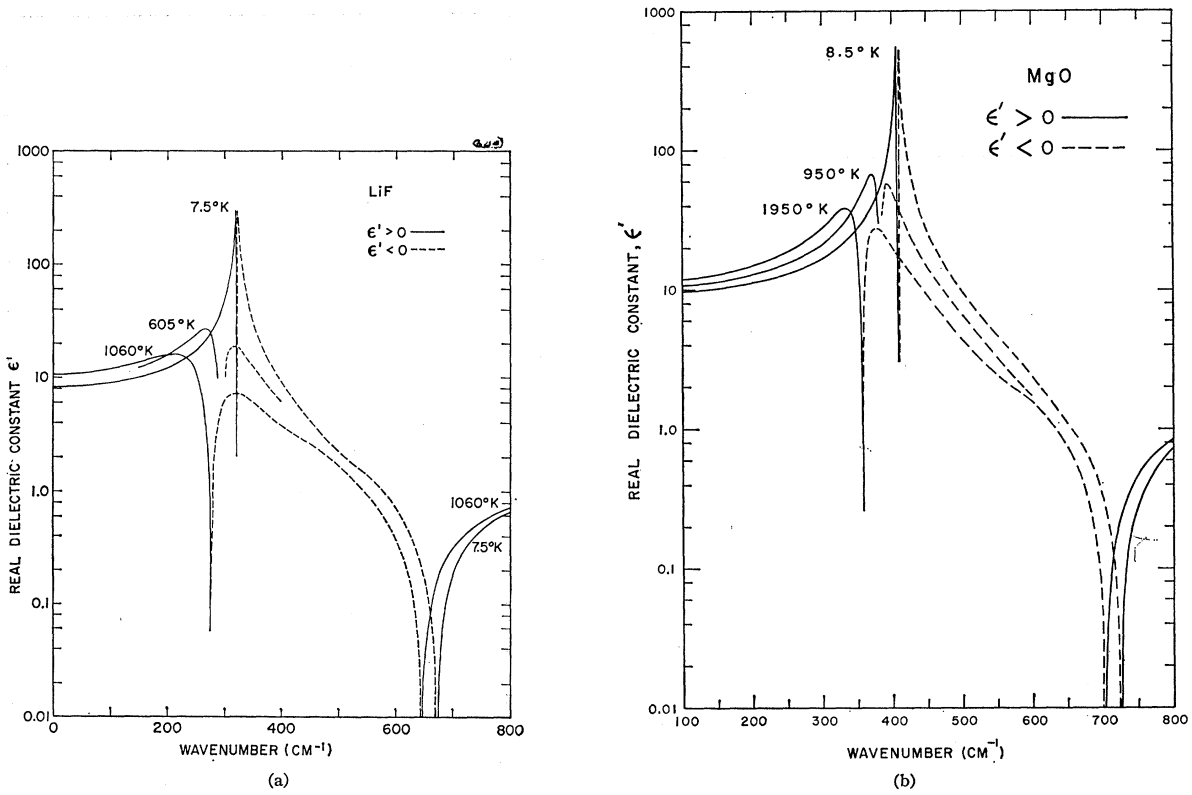

FIG. 8. Real part of complex dielectric constant of LiF and MgO as function of wave number and temperature. Dashed lines are the regions of negative dielectric constants.

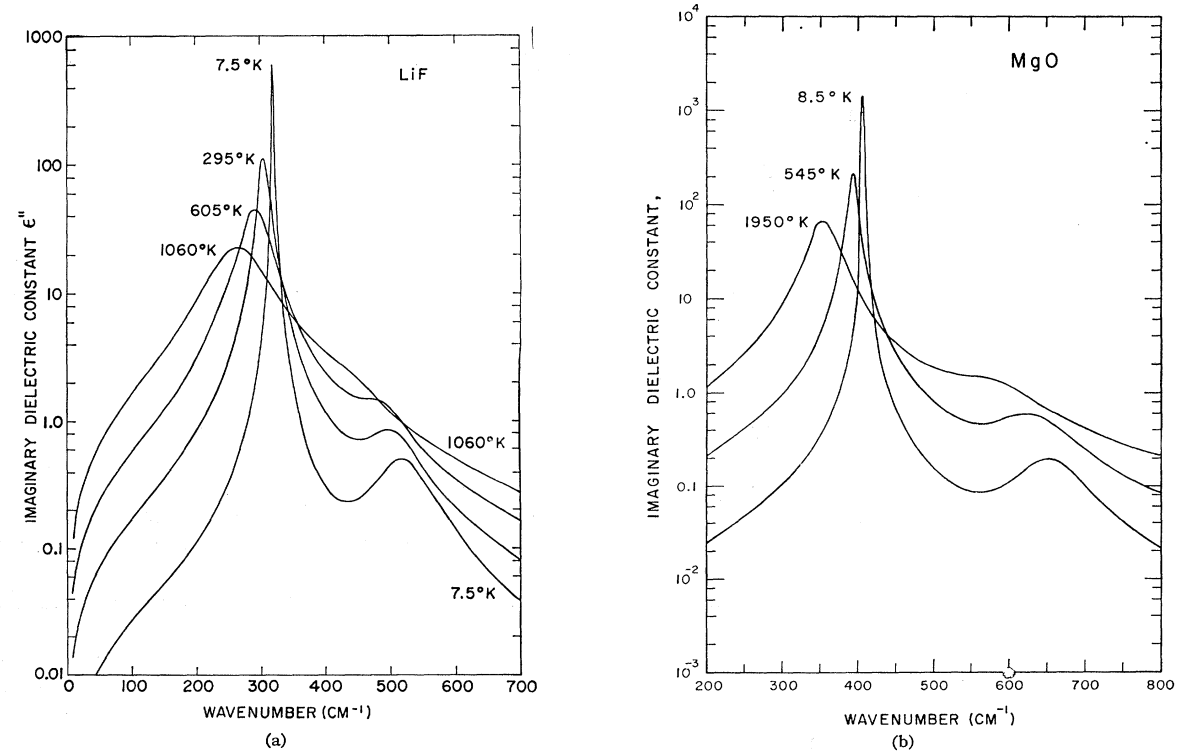

FIG. 9. Imaginary part of complex dielectric constant of LiF and MgO as function of wave number and temperature.

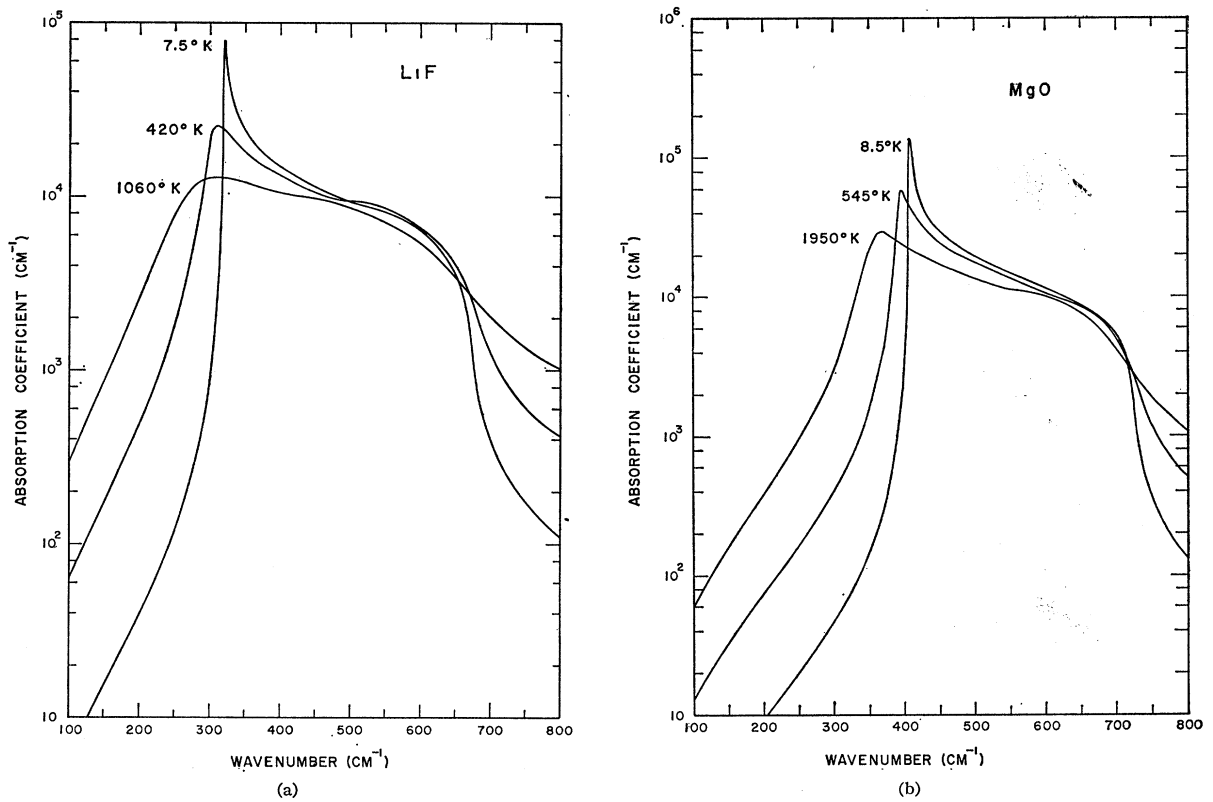

FIG. 10. Absorption coefficient of LiF and MgO as function of wave number and temperature.

the form

$$\epsilon_{\mu\nu}=\delta_{\mu\nu}+4\pi\chi_{\mu\nu}. \tag{4}$$

There have been several attempts to calculate the optical constants of a dielectric crystal along these lines.[22–25] They do not all lead to identical results, however. The major theories we will discuss are those of Born-Huang,[22] Maradudin-Wallis,[23] and Mitskevich.[24]

In the Born-Huang treatment a Hamiltonian is assumed which contains quadratic and cubic terms in the crystalline potential and an interaction term through which the electric field couples to the dipole moment of the vibrating lattice. This Hamiltonian was designed to represent, in the first order, an ionic crystal like one of the alkali halides. Their expression for the dielectric susceptibility involves a frequency and temperature-dependent damping constant $\gamma(\nu,T)$ such that when the susceptibility is evaluated at $\nu=\nu_1$ and second-order contributions are dropped, one finds

$$\mathrm{Im}\chi(\nu,T)\,|_{\nu=\nu_1}\sim[\bar{\gamma}(\nu_1,T)]^{-1}. \tag{5}$$

Here, the susceptibility tensor reduces to a scalar for cubic crystals and is dominated by its imaginary part. $\bar{\gamma}$ represents some effective or averaged damping constant. Born and Huang also find that in the high-temperature limit ($kT>h\nu_1$) the imaginary part of χ decreases inversely as the cube of the temperature in the center of the dispersion region.

The model for ionic crystals proposed by Mitskevich employs a Hamiltonian which contains several Born-Mayer type potentials with parameters to be determined by comparison to experiment. In this calculation of the dielectric constant Mitskevich includes contributions from higher order electric moments as well as 3rd and 4th order anharmonic terms. He obtains the following form for the dielectric constant in a cubic, ionic crystal:

$$\epsilon(\omega,T)=\epsilon_\infty+\frac{(\epsilon_0-\epsilon_\infty)\Omega_0^2}{\Omega_\omega^2-\omega^2+i\gamma(\omega,T)\omega}. \tag{6}$$

Here Ω_ω is the "dispersion frequency," $\gamma(\omega,T)$ is the damping constant and Ω_0 is a constant. The form of $\epsilon(\omega,T)$ is close to the classical Drude dispersion formula except that the damping constant is now a function of both frequency and temperature. Mitskevich has computed the cubic and fourth-order contributions of the crystalline potential to γ in the high-temperature limit

[22] M. Born and K. Huang, *Dynamical Theory of Crystal Lattices* (Oxford University Press, New York, 1954).
[23] A. A. Maradudin and R. F. Wallis, Phys. Rev. **125**, 4 (1962).
[24] V. V. Mitskevich, Fiz. Tverd. Tela **4**, 3035 (1962) [English transl.: Soviet Phys.—Solid State **4**, p. 2224 (1963)].
[25] J. Neuberger and R. D. Hatcher, J. Chem. Phys. **34**, 5 (1961).

and obtained

$$\gamma_3(\omega,T)\sim\frac{T}{\omega_1^4}\phi_3(\omega), \tag{7}$$

$$\gamma_4(\omega,T)\sim\frac{T^2}{\omega_1^6}\phi_4(\omega), \tag{8}$$

where ω_1 is the transverse optical mode at the center of the Brillouin zone. The $\phi_3(\omega)$ and $\phi_4(\omega)$ are functions of frequency which depend on sums over the density of phonon states in wave-vector space. Strictly speaking, the theory of Mitskevich is not completely quantum mechanical since it does not make use of the full operator formalism in treating the phonons and the electromagnetic field. It is interesting to note that Neuberger[25] performed a similar calculation including only the cubic terms in the potential and found results similar to Eqs. (6) and (7) where the frequency dependence of γ was also computed from the density of phonon states.

Perhaps the most rigorous quantum-mechanical treatment of the problem is the theory proposed for ionic crystals by Maradudin and Wallis. They make full use of the operator formalism of quantum-field theory and the density matrix approach in treating quantum statistical aspects of the problem. They develop the operator equations of motion of a suitably transformed set of normal coordinates, and the associated equations for the damping constant. Approximate solutions to these operator equations are obtained and the general formalism of Kubo[26] is used to calculate the electric-susceptibility tensor. They obtain the following general result for the dielectric susceptibility:

$$\chi_{\mu\nu}=(2V_0)^{-1}\sum_j\frac{M_{\mu j}M_{\nu j}}{\omega(0j)}\left\{\frac{1}{\omega+\omega(0j)+\Delta\omega(0j)+i\gamma(0j)}-\frac{1}{\omega-\omega(0j)-\Delta\omega(0j)-i\gamma(0j)}\right\}, \tag{9}$$

where the γ is given by

$$\gamma(0j)=\frac{h}{4}\sum_{k'j'k''j''}\frac{|V(0j;k'j';k''j'')|^2}{\omega(0j)|\omega(\mathbf{k}'j')|\omega(\mathbf{k}''j'')}\times(n_{k'j'}+\tfrac{1}{2})\delta[\omega-\omega(\mathbf{k}'j')-\omega(\mathbf{k}''j'')] \tag{10}$$

and

$$n_{k'j'}=\left[\exp\left(\frac{\hbar|\omega(\mathbf{k}'j')|}{kT}\right)-1\right]^{-1}.$$

Here, j refers to the jth optical branch, $\mathbf{k}$ is a wave vector, the V's are the cubic parts of the Hamiltonian when it is re-expressed in terms of the normal coordinates, and the $\Delta\omega$'s are the frequency shifts. The form of γ shows that the phonons are coupled together through the cubic terms in the Hamiltonian which produces damping of main resonance. We also note that a complete calculation of the frequency dependence of γ would mean knowledge of the density of phonon states in wave vector space for the particular crystal concerned.

There are two comments we want to make about dielectric dispersion theory. The first point is that a simple extension of the classical Drude formula to a superposition of several poles (ν_j's) each having a frequency-independent damping constant is not rigorously equivalent to any of the results obtained by the above theories. According to the pole-fit procedure the susceptibility of an ionic crystal may be represented by

$$4\pi\chi=\epsilon_\infty+\sum_{j=1}^{n}\frac{4\pi\rho_j}{1-(\nu/\nu_j)^2-i(\gamma_j/\nu_j)(\nu/\nu_j)}. \tag{11}$$

If we believe in quantum mechanical dispersion theory, for instance, the one proposed by Maradudin and Wallis, then we might regard Eq. (11) as a distribution of poles with a constant amount of damping in an effort to approximate the unknown (or at least uncertain) frequency behavior of the γ appearing in the quantum-mechanical treatments. In light of all this it is indeed surprising that Eq. (11) fits the experimental data as well as it does.

The second point we wish to make is that if we evaluate all of the above theories at $\nu=\nu_1$ we obtain essentially the same result. Evaluating the Maradudin-Wallis results at the center of the dispersion region ($\nu=\nu_1$) we obtain for a cubic, ionic type crystal:

$$\chi|_{\nu=\nu_1}\sim\nu_1^{-1}(T)\left\{\frac{1}{2\nu_1(T)+i\gamma}-\frac{i}{\gamma}\right\}. \tag{12}$$

Using the approximation that $\nu_1\gg\gamma(\nu,T)$ we see that the imaginary part of χ is the same as that given by (5) obtained from the Born and Huang theory to within a phase factor. We also note that the imaginary part dominates the susceptibility in this region and is several orders of magnitude greater than the real part of χ at $\nu=\nu_1$. The other quantum theories, even though they differ in form from one another, give the same form for the imaginary part of χ to within a phase factor when evaluated at $\nu=\nu_1$. If we examine the classical pole-fit formula (Eq. 11) at $\nu=\nu_1$ we see that the main pole dominates the sum and we have for χ

$$4\pi\chi|_{\nu=\nu_1}=\epsilon_\infty+i(4\pi\rho_1/\nu_1)\gamma^{-1}.$$

Substituting some known quantities into this expression we find that the classical dispersion formula evaluated at $\nu=\nu_1$ yields a susceptibility which is again dominated by its imaginary part and given by Eq. (5). It may be mentioned here that recently Cowley[27] obtained results

[26] R. Kubo, J. Phys. Soc. Japan 12, 570 (1957).

[27] R. A. Cowley, Advan. Phys. 12, 421 (1963).

similar to Maradudin and Wallis by considering the shift and the damping small compared to $\omega(0j)$.

All the representations of χ including the classical pole-fit procedure give essentially the same results when evaluated at $\nu=\nu_1$. It is therefore valid to use the simple pole-fit procedure of classical dispersion theory when evaluated at the center of the dispersion region in order to draw some conclusions about the quantum mechanical quantities at $\nu=\nu_1$. If a quantitative estimate is made, we find that the imaginary parts of Eqs. (6), (9), and (11) are actually equivalent at $\nu=\nu_1$ to within less than 1%. We want to emphasize again that the results of Born and Huang, Mitskevich, Maradudin and Wallis and the classical pole-fit all differ from one another in the wings of the absorption. Therefore, it may not be valid to draw definite conclusions about the behavior of χ derived from a pole-fit analysis (and hence the optical constants n and k) in these regions of the spectrum.

V. DEPENDENCE OF DAMPING FACTOR ON TEMPERATURE

If we examine Eq. (10) given by Maradudin and Wallis for the damping constant it suggests that when evaluated at $\nu=\nu_1$ we expect γ to have the form

$$\left.\frac{\gamma(\nu,T)}{\nu_1}\right|_{\nu=\nu_1}=\frac{\text{constant}}{\nu_1^4}\left[\left(\exp\frac{h\nu_1}{kT}-1\right)^{-1}+\frac{1}{2}\right], \quad (13)$$

where the constant represents an average value from the summation. We know from the data presented in Sec. III that ν_1 depends on the temperature and for LiF has an average coefficient given by

$$\nu_1(T)\simeq 320(1-\alpha T)\ \text{cm}^{-1},$$

where

$$\alpha\simeq 1.45\times 10^{-4}\ \text{cm}^{-1}\ \text{per}\ ^\circ\text{K}.$$

We see that from room temperature up to 1060°K the reststrahlen frequency in LiF decreases linearly by about 13%. It is difficult to know whether or not there is any temperature dependence buried in the constant factor shown in Eq. (13). However, other calculations of γ in the high-temperature limit ($kT>h\nu_1$) suggest that γ/ν_1 is proportional to T/ν_1^5 which is consistent with Eq. (13). A graph of the damping constant for the main band in LiF and MgO as a function of temperature is shown in Fig. 5. For LiF, kT is about 3 times $h\nu_1$ at 1060°K, and for MgO, kT is about 4 times $h\nu_1$ at 1950°K. The effective temperature dependence of γ_1/ν_1 for LiF is about $T^{3/2}$ and for MgO about T. Now we notice that Eq. (13), suggested by the Maradudin-Wallis theory (also Mitskevich and Neuberger in the high temperature limit) appears to contain a $\nu_1(T)^{-4}$ multiplicative term which would tend to make the temperature dependence of γ_1/ν_1 more than the first power of T when $kT>h\nu_1$. A similar result would hold for MgO only to a lesser extent because the coefficient

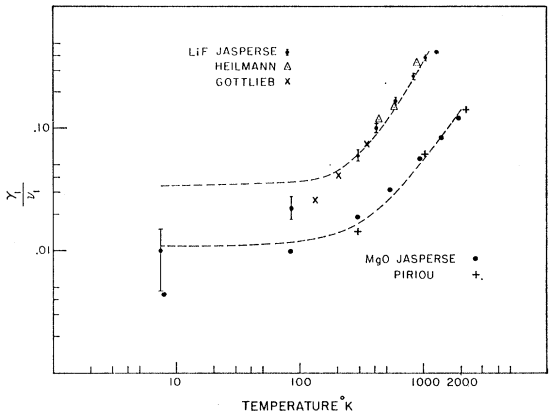

FIG. 11. Theoretical-curve fit of Eq. (13) to the experimentally-determined damping constant.

$d\nu_1/dT$ for MgO is about ½ of that for LiF. Figure 11 shows the same data as Fig. 5 except that the dotted line in Fig. 11 represents a curve fit of the experimental data to Eq. (13). Data reported by Heilmann[17] and Gottlieb[8] for LiF and by Piriou[13,14] for MgO are also included in this graph. Equation (13) fits the data reasonably well at high temperatures but deviates at the lower temperatures. It is true that the experimental error associated with γ_1/ν_1 increases rapidly at low temperatures but the theoretical expression (curve fitted at the higher temperatures) appears to lie well outside of the estimated error. The Born-Huang theory predicts that at the center of the resonance, γ_1/ν_1 varies in proportion to the cube of the temperature in the high temperature limit. This dependence seems to be much stronger than is indicated by experiment. The high-temperature limit of the Maradudin-Wallis results and the treatments by Neuberger[25] and Blackmann[28] in which each mode of vibration in the crystal is assigned an energy kT, produce similar results, and agree reasonably well with Eq. (13). We note that Hass found that the damping constant of NaCl in the high temperature limit was proportional to a power of T slightly less than two.[29] It is plausible that his results could also be explained by Eq. (13) and a temperature dependence in ν_1 even stronger than the one we observe for LiF.

The behavior of $\gamma(\nu_1,T)$ at low temperatures ($kT\ll h\nu_1$) as suggested by Eq. (13) is dominated by the constant ½ inside the brackets. The ½ is there as a result of the fact that quantum oscillators are believed to have zero-point energy in their ground state. If the ½ were not present then the damping constant would go to zero exponentially with decreasing temperature. In Fig. 11, we see that if Eq. (13) is curve-fitted at high temperatures (because of the fact that experimental errors in γ are less there) then the theoretical curve deviates from the experimental values at low tem-

[28] M. Blackmann, Trans. Roy. Soc. (London) **A236**, 103 (1936).
[29] M. Hass, Phys. Rev. **117**, 6 (1960).

peratures. This is confirmed not only by the data presented in part III of this paper but also by the data on LiF reported by others and included in Fig. 11. It is perhaps unjustified to make any firm conclusion about the discrepancy between experiment and Eq. (13) at low temperatures even though the vertical bars on Fig. 11 represent our best estimates of experimental error. The experimental values for γ at these low temperatures are quite sensitive to the 98.5% reflectivity assumed for the aluminized reference mirror, to which all measurements are compared. We can say, however, that the experimentally determined damping constant evaluated at ν_1 has a definite bend at lower temperatures which suggests that γ does not vanish as the temperature becomes arbitrarily small.

VI. ABSORPTION IN THE WINGS OF THE DISPERSION REGION

We have seen in Sec. IV that the classical pole-fit procedure, in general, gives a different formula for the dielectric constant than a quantum mechanical treatment of the problem. The results are essentially the same at the center of the dispersion region but differ substantially in form in the wings of the absorption region. Even though we are uncertain whether or not the pole-fit procedure is valid in the wings of the absorption region, some comments about absorption here are appropriate. According to a quantum-mechanical treatment, continuous absorption is produced by a coupling of the phonons arising from the presence of cubic or higher order terms in the crystalline potential or higher order terms in the expansion of the electric moment. If the cubic terms only are considered, then we may visualize two phonon processes which produce an absorption continuum with a peak near the reststrahlen frequency. Absorption may occur in the following two ways if cubic terms are present in the potential: A photon is absorbed and two phonons are created (a summation process), or a photon is absorbed, annihilating an existing phonon and creating another phonon (a difference process).

Figure 12 shows a log-log graph of the extinction coefficient as a function of temperature evaluated in the wings of the absorption region. The two solid lines represent the values of k calculated from the pole-fit procedure and the experimental data shown in the graph were reported in the literature as direct measurements of the extinction coefficient. The upper curve is the extinction coefficient evaluated at $\nu=\nu_2(T)$ and is on the high frequency side of ν_1. The data reported by Heilmann[17] are shown on the graph and agree with the results of pole-fit procedure in this region of the spectrum. We do note, however, that large errors in the reflectivity in this region of the spectrum produce only very small changes in the calculated values of k. We see that the temperature dependence of the absorption here is very slight, decreasing slightly with

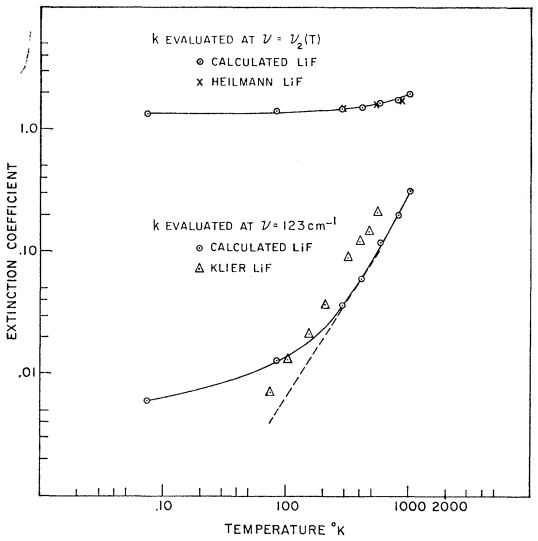

FIG. 12. Absorption in the wings as a function of temperature for LiF.

decreasing temperature. We also note that the temperature coefficient of $\nu_2(T)$ for both LiF and MgO is about twice that of $\nu_1(T)$. This evidence would tend to support the conjecture that absorption on the high frequency side of ν_1 comes about because of summation processes. The lower curve in Fig. 12 shows the calculated values of k (solid line) evaluated at a fixed frequency (123 cm^{-1}). Data reported by Klier[10] are also plotted on this graph with the band at 110 μ subtracted out. This must be done in order to compare to our pole-fit results since our measurements did not extend to the far infrared. However, as discussed in Sec. III one must be careful in comparing to the results obtained by Klier. We only do so here to examine the major trend shown in the data. We see that both the pole-fit results and the direct measurements of k evaluated at 123 cm^{-1} show a very strong temperature dependence, decreasing rapidly as the temperature is decreased. This result would support the theory that difference processes produce the absorption on the low-frequency side of ν_1. In addition, the pole-fit results suggest a leveling off in the values of k at very low temperatures which, in turn, implies a finite amount of absorption in the wings of the absorption region as the temperature becomes arbitrarily small.

There has been considerable discussion in the literature concerning the origin of the side bands observed in the reflection spectra of the alkali halides. There are two mechanisms proposed in the literature to explain the occurrence of these side bands. The two possible explanations are the anharmonic mechanism of phonon coupling discussed by several of the previously referenced authors[22–25] and the charge-deformation mechanism proposed by Lax and Burstein.[30] In the anharmonic

[30] M. Lax and E. Burstein, Phys. Rev. 97, 1 (1955).

theory, subsidiary maxima could arise from a two-phonon process at critical points $[\nabla_k\omega(\mathbf{k})=0]$ in the phonon dispersion relations where the density of phonon states is large. This effect would then enter through frequency dependence of the quantum damping constant in such a way as to produce a local maximum in the values of k. It is generally agreed that the Lax-Burstein theory is the most likely model to explain infrared absorption in homopolar crystals where the dipole moment is absent. However, whether the side band observed in the alkali halides comes about because of the higher order terms in the expansion of the electric moment or the anharmonic terms in the expansion of the crystalline potential is an open question. If we examine the Lax-Burstein model in detail, we find that they predict the existence of a subsidiary peak in the absorption spectrum for an alkali-halide type crystal in the vicinity of $\nu=\sqrt{2}\nu_1$. The Lax-Burstein theory also suggests that the extinction coefficient evaluated at ν_2 should be proportional to at least the square of the temperature in the high temperature limit. The data shown by Heilmann in Fig. 12, which represents a direct measurement of k, and the classical pole-fit analysis give roughly the same values for k and show only a very slight temperature dependence in this region of the spectrum.

In many alkali halides the occurrence of the sidebands approximately at the position of the $\mathbf{k}\simeq 0$ longitudinal optical mode may tempt one to conclude that perhaps it occurs by means of the process described by Berreman[15] due to finite convergence of the incident beam encountered in most experimental situations. However, in the cases of LiF and MgO, ν_2 is distinctly different from ν_l calculated either from the Lyddane-Sachs-Teller relation or from the Drude method,[1] as may be seen in Tables I and II.

VII. SHIFT OF FREQUENCY WITH TEMPERATURE

A. General Remarks

It is generally believed that the change in peak position and the width of the infrared active lattice modes are caused by anharmonic forces in the crystal lattice. The width and temperature shift of the infrared active lattice modes are the same as the phonon width and shift which may also be observed in other types of experiments, e.g., neutron scattering, vibronic fine structure or Raman scattering. Maradudin[31] and Maradudin and Fein[32] have treated the problem of scattering of neutrons by an anharmonic crystal. They obtained the one-phonon scattering cross section for the coherent scattering of thermal neutrons by retaining the cubic and quartic anharmonic terms in crystal's Hamiltonian. These treatments, although derived for neutron scattering, may also be applied to other experiments involving phonon life times, as has been indicated by Loudon[33] for the Raman scattering. The expressions for the frequency shift and the width of one phonon lines given by Maradudin and Fein are too complicated to be evaluated explicitly, except for very idealized Bravais lattices. However, from the expressions they have given it is clear that the magnitudes of the shift should increase with temperature, the dependence being linear for $T\geq\Theta$, where Θ is the Debye temperature of the crystal. The change of the one-phonon frequency with temperature is not entirely due to the anharmonic coupling of the phonon in question with other phonons, but also due to the thermal expansion of the crystal. As a matter of fact, in many instances, the two effects, namely the anharmonic coupling and the thermal expansion, may have opposite temperature dependencies, one increasing while the other decreasing. Cowley[27] has calculated the shift for KBr and NaI by using phenomenological anharmonic potentials consistent with the experimentally known dispersion curves for these two crystals. In what follows, we shall present expressions for the volume dependence of the long wavelength transverse and longitudinal optical (TO and LO) modes of an ionic crystal, and in view of the fact that no experimental dispersion curve exists for LiF, MgO, and RbI, we shall only qualitatively discuss the various factors that contribute to the shifts of the $\mathbf{k}\simeq 0$ TO modes of these crystals.

B. Volume Dependence of One-Phonon Frequency

If a normal mode of frequency ν_i is purely a function of volume V, one may write

$$\gamma_i=-\frac{1}{3\alpha}\frac{1}{\nu_i}\left(\frac{\partial\nu_i}{\partial T}\right)_P, \tag{14}$$

where γ_i is the Grüneisen parameter for the ith mode [note here that γ_i is not related to the damping constant defined by Eq. (1)] given by

$$\gamma_i=-d\ln\nu_i/d\ln V, \tag{15}$$

and 3α is the volume thermal expansion coefficient. Rewriting Eq. (14) in terms of the mode-frequency ν_i as a function of temperature one has at constant pressure

$$\ln\nu_i(T)=\ln\nu_i(0)-3\gamma_i\int_0^T\alpha dT, \tag{16}$$

where $\nu_i(T)$ and $\nu_i(0)$ are the frequencies of the ith mode at temperatures T and 0°K, respectively. If γ_i for the mode was known the shift of the mode frequency ν_i with T due to thermal expansion of the crystal may be obtained from Eq. (16).

An estimate of γ_i is possible from the Born and Huang theory of the long wavelength optical modes in ionic crystals. The expression for the $\mathbf{k}\simeq 0$ TO mode is

[31] A. A. Maradudin, Phys. Status Solidi, **2**, 1493 (1963).
[32] A. A. Maradudin and A. E. Fein, Phys. Rev. **128**, 2589 (1962).
[33] R. Loudon, Advan. Phys. **13**, 423 (1964).

given by[34]

$$-\omega_t^2=-\frac{f}{\mu}+\frac{(4\pi/3)(e^2/\mu V_a)}{1-(4\pi/3)[(\alpha_+ +\alpha_-)/V_a]}, \quad (17)$$

in which f is the nearest-neighbor force constant, μ the reduced mass per ion pair and $V_a=2r_0^3$ the Bravais unit cell volume, where r_0 is the nearest-neighbor distance, and α_+ and α_- are the ionic polarizabilities. By using the Lyddane-Sachs-Teller relation[35] a similar expression for ω_l the long-wavelength LO mode may also be obtained.

The force constant f may be evaluated by using the Born-Mayer potential

$$u=-\alpha e^2/r+Mbe^{-\sigma(r/r_0)}, \quad (18)$$

where α is the Madelung constant, M the coordination number and b and σ are potential constants. f may then be shown[36] to be

$$f=\tfrac{1}{3}(\sigma-2)\alpha e^2/r_0^3. \quad (19)$$

For the Grüneisen parameters one therefore obtains

$$\gamma_t=\frac{(f/\sigma)[(\sigma^2-2\sigma-2)/(\sigma-2)]-\pi e^2/3r_0^3}{f-2\pi e^2/3r_0^3} \quad (20)$$

and

$$\gamma_l=\frac{(f/\sigma)[(\sigma^2-2\sigma-2)/(\sigma-2)]+2\pi e^2/3r_0^3}{f+4\pi e^2/3r_0^3}. \quad (21)$$

In the above expressions it has been assumed that the ions are rigid, i.e., $\alpha_+=\alpha_-=0$. However, for the more realistic case of polarizable ions one may use the Clausius-Mossoti relation[37]

$$\tfrac{4}{3}\pi(\alpha_+ +\alpha_-/V_a)=(\epsilon_\infty-1)/(\epsilon_\infty+2) \quad (22)$$

to obtain

$$\gamma_t=\frac{(f/\sigma)[(\sigma^2-2\sigma-2)/(\sigma-2)]-\frac{1}{3}\pi[(\epsilon_\infty+2)/3](e^2/r_0^3)}{f-\frac{2}{3}\pi[(\epsilon_\infty+2)/3](e^2/r_0^3)} \quad (23)$$

and

$$\gamma_l=\frac{(f/\sigma)[(\sigma^2-2\sigma-2)/(\sigma-2)]+\frac{2}{3}\pi[\epsilon_\infty+2)/3](e^2/r_0^3)}{f+\frac{4}{3}\pi[(\epsilon_\infty+2)/3](e^2/r_0^3)}. \quad (24)$$

Expressions for γ_t and γ_l may also be obtained by using a potential function involving an inverse power type of repulsive energy of the form

$$u=-\alpha e^2/r+Mb/r^n. \quad (25)$$

γ_t and γ_l are given by

$$\gamma_t=\frac{(f/\sigma)(n+2)-\frac{1}{3}\pi(e^2/r_0^3)}{f-\frac{2}{3}\pi(e^2/r_0^3)}, \quad (26)$$

and

$$\gamma_l=\frac{(f/\sigma)(n+2)+\frac{2}{3}\pi(e^2/r_0^3)}{f+\frac{4}{3}\pi(e^2/r_0^3)} \quad (27)$$

for the rigid ion approximation. For polarizable ions one obtains

$$\gamma_t=\frac{(f/\sigma)(n+2)-\frac{1}{3}\pi[(\epsilon_\infty+2)/3](e^2/r_0^3)}{f-\frac{2}{3}\pi[(\epsilon_\infty+2)/3](e^2/r_0^3)}, \quad (28)$$

and

$$\gamma_l=\frac{(f/\sigma)(n+2)+\frac{2}{3}\pi[(\epsilon_\infty+2)/3](e^2/r_0^3)}{f+\frac{4}{3}\pi[(\epsilon_\infty+2)/3](e^2/r_0^3)}. \quad (29)$$

In expressions (26)–(29) f is given by

$$f=(n-1)\alpha e^2/3r_0^3. \quad (30)$$

In Table III, γ_t and γ_l are evaluated from Eqs. (20, 21, 23, 24, 26, 27–29) for LiF, RbI, and MgO. It may be seen from Table III that in all the cases γ_t is approximately three times γ_l indicating a stronger temperature dependence of the $k\simeq 0$ TO mode as compared to the LO mode, which is also borne out by our experimental results presented in Tables I and II.

C. Comparison with Experiment

In this section we discuss the shift of the long wavelength TO mode of LiF and MgO with temperature as revealed from our reflection studies. Also included in the discussion is the effect of temperature on the $k\simeq 0$ TO mode of RbI, experimental data for which have been reported by Jones *et al.*[38] from transmission measurements.

We define the observed shift in the frequency as

$$\Delta\nu_{\text{obs}}=\nu_t(0)-\nu_t(T), \quad (31)$$

where $\nu_t(0)$ and $\nu_t(T)$ are the observed one-phonon resonance frequencies at 0°K and T°K, respectively. $\nu_t(0)$ is obtained from the extrapolation of low-temperature data. The third law of thermodynamics demands that the thermal expansion vanish as $T\to 0$, consequently ν_t should approach a constant value as $T\to 0$, by virtue of Eq. (14). This is more so because at very low temperatures the anharmonic effects also tend to diminish. Although the LO mode exhibit this tendency in both MgO and LiF, the TO modes for these do not

[34] M. Born and K. Huang, *Dynamical Theory of Crystal Lattices* (Oxford University Press, London, 1954) p. 106.
[35] R. H. Lyddane, R. G. Sachs, and E. Teller, Phys. Rev. **59**, 673 (1941).
[36] S. S. Mitra and S. K. Joshi, Physica **26**, 284 (1960).
[37] Reference 35, Chap. II.
[38] G. O. Jones, D. H. Martin, P. A. Mawer, and C. H. Perry, Proc. Roy. Soc. (London) **A261**, 10 (1961).

TABLE III. Grüneisen parameter for the long-wavelength optical modes of LiF, RbI, and MgO.

Crystal	σ[a]	η[b]	Rigid ion Born-Mayer γ_t	Rigid ion Born-Mayer γ_l	Rigid ion Eq. (25) γ_t	Rigid ion Eq. (25) γ_l	Polarizable ion Born-Mayer γ_t	Polarizable ion Born-Mayer γ_l	Polarizable ion Eq. (25) γ_t	Polarizable ion Eq. (25) γ_l
LiF	8.25	6.0	2.44	0.88	3.46	0.84	3.76	0.83	4.51	0.80
RbI	10.4	11.0	2.61	1.14	3.12	1.47	3.02	1.05	3.52	1.21
MgO[c]	14	13	3.03	1.64	3.30	1.77	3.90	1.42	4.30	1.52

[a] Data from Ref. 34 (p. 26).
[b] Data from F. Seitz, *The Modern Theory of Solids* (McGraw-Hill Book Company, Inc., New York, 1940), p. 80.
[c] σ and η for MgO are obtained from Eqs. (17), (19), and (30) using the extrapolated 0°K ω_t and ϵ_∞ from our measurements.

seem to approach a stationary value even at very low temperatures. This we believe is due to the way the TO mode for these crystals is derived, viz. from the multi-resonance damped oscillator fit of reststrahlen bands, the limitations of which were discussed in Sec. III. For RbI direct-transmission measurements,[38] on the other hand, show the expected tendency.

To separate out the contribution of thermal expansion to observed $\Delta\nu$ we define

$$\Delta\nu_G=\nu_t(0)-\nu_G. \tag{32}$$

ν_G the $\mathbf{k}\simeq 0$ TO mode in the Grüneisen approximation is given by [see Eq. (16)]

$$\nu_G=\nu_t(0)\exp\left(-3\gamma_t\int_0^T \alpha dT\right). \tag{16a}$$

TABLE IV. Grüneisen and anharmonic contributions to the frequency shift of the $\mathbf{k}\simeq 0$ TO mode in LiF.[a,b]

T°K	ν_G (cm^{-1})	$\Delta\nu_G$ (cm^{-1})	ν_{obs} (cm^{-1})	$\Delta\nu_{obs}$ (cm^{-1})	$\Delta\nu_{AN}$ (cm^{-1})
100	319	1	315	5	4
200	312	8	310	10	2
300	301	19	306	14	−5
500	276	44	298	22	−22
700	249	71	289	31	−40
900	219	101	279	41	−60
1100	188	132	269	51	−81

[a] Thermal-expansion data used in the calculation of ν_G are from *American Institute of Physics Handbook* (McGraw-Hill Book Company, Inc., New York, 1957), 2nd ed., p. 4–73.
[b] γ_t used is the average of that from columns 8 and 10 of Table III.

TABLE V. Grüneisen and anharmonic contributions to the frequency shift of the $\mathbf{k}\simeq 0$ TO mode in MgO.[a,b]

T°K	ν_G (cm^{-1})	$\Delta\nu_G$ (cm^{-1})	ν_{obs} (cm^{-1})	$\Delta\nu_{obs}$ (cm^{-1})	$\Delta\nu_{AN}$ (cm^{-1})
100	408	0	405	3	3
200	406	2	402	6	4
300	402	6	400	8	2
600	385	23	392	16	−7
900	367	41	383	25	−16
1400	335	73	368	40	−33
1900	304	104	356	52	−52

[a] Thermal-expansion data used in the calculation of ν_G are from A. Goldsmith, H. J. Hirschhorn, and T. E. Waterman, Wright Air Development Center WADC Technical Report No. 58-476, 1960, Vol. III, (unpublished).
[b] γ_t used is the average of that from columns 8 and 10 of Table III.

The anharmonic part of $\Delta\nu$ is then obtained as

$$\Delta\nu_{AN}=\Delta\nu_{obs}-\Delta\nu_G. \tag{33}$$

In Tables IV and V are presented $\Delta\nu_G$ and $\Delta\nu_{AN}$ for LiF and MgO obtained in the fashion outlined in the foregoing. In the high-temperature limit ($T\geq\Theta$) it may be seen that for both LiF and MgO the anharmonic contribution is in the opposite direction relative to the volume effect, as predicted by the Maradudin and Fein theory. The quartic term in the anharmonic potential makes a much larger contribution to the shift than the cubic term. Whereas, the Grüneisen contribution and the small cubic anharmonic contribution are in one direction (decreasing frequency with increasing temperature) the quartic anharmonic contribution is in the opposite direction. The first two contributions to the shift are in the direction of the observed shift, which is smaller than the value predicted by these two contributions alone. Compensation occurs through the third contribution. The combined anharmonic contribution ($-\Delta\nu_{AN}$) is plotted against temperature in Figs. 13 and 14 for LiF and MgO, respectively. As predicted by the Maradudin and Fein theory, in the high-temperature limit, $\Delta\nu_{AN}$ indeed varies linearly with temperature.

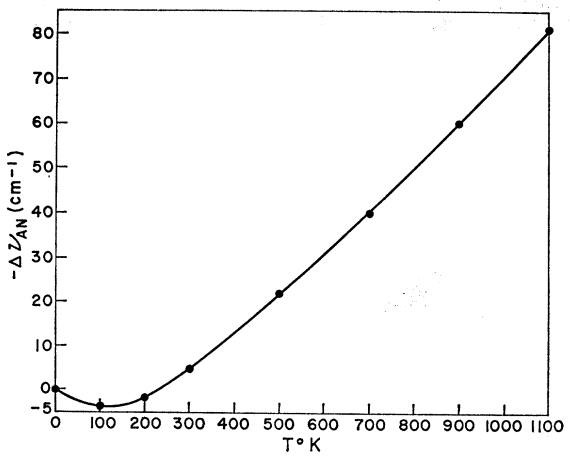

FIG. 13. Anharmonic contribution to the shift of $\mathbf{k}\simeq 0$ TO mode of LiF as a function of temperature.

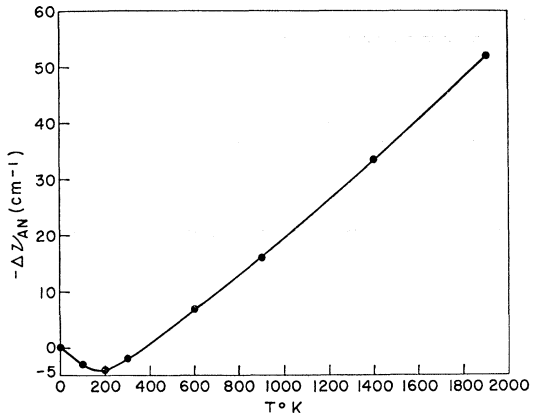

FIG. 14. Anharmonic contribution to the shift of k≃0 TO mode of MgO as a function of temperature.

For KBr and NaI the anharmonic contribution to the shift has been calculated by Cowley using a phenomenological potential. In Figure 15, his calculated data for KBr and NaI are compared with our data derived from the observed shifts in LiF and MgO in suitable reduced coordinates. The general similarity of the curves with

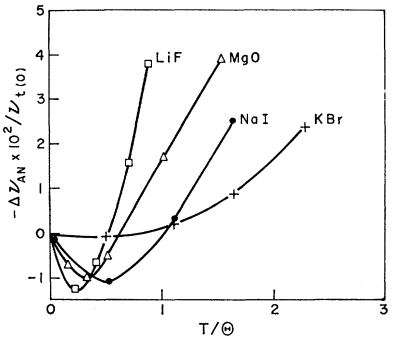

FIG. 15. Anharmonic contribution to the shift as a function of reduced temperature T/Θ where $\Theta=(h/k)\nu_t(0)$. square: LiF; triangle: MgO; circle: NaI; and plus sign: KBr. LiF and MgO: experimental data; NaI and KBr: calculated by Cowley.

the linear portions extrapolated to about $T\sim\Theta$ is a further testimony to the qualitative agreement with the Maradudin and Fein theory. The strong behavior of LiF may be traced back to its unusual variation of thermal expansion coefficient with temperature.

In the case of RbI the infrared data exist only over a small temperature range (up to 300°K). Using the thermal-expansion data of Schuele and Smith,[39] ν_G for this crystal has been calculated. Within the experimental error (0.5 cm^{-1}), they agree with the observed frequency, as shown in Fig. 16, indicating that the volume dependence of the frequency almost entirely

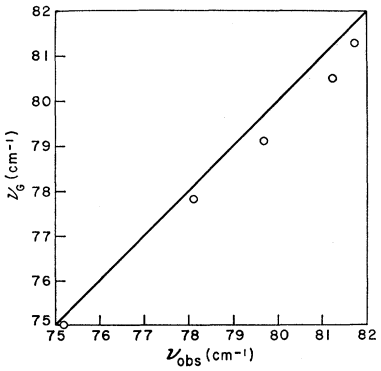

FIG. 16. Transverse - optic - mode frequency of RbI. Comparison of observed value with that calculated from Eq. (16a) at various temperatures (4°K to 300°K).

accounts for the observed shift over the range of temperature considered, and that the anharmonic contributions are negligibly small.

ACKNOWLEDGMENTS

The authors wish to thank L. C. Mansur for his help in data evaluation and computation, and E. P. Marram for experimental assistance and his involvement in the computer analysis. Thanks are also due to O. M. Clark for his experimental contribution to the program.

[39] D. E. Schuele and C. S. Smith, J. Phys. Chem. Solids **25**, 801 (1964).